# Homework 3 in EL2450 Hybrid and Embedded Control Systems

First name1 Last name1
person number
email

First name2 Last name2
person number
email

First name3 Last name3
person number
email

First name4 Last name4
person number
email

## Task 1

$$\begin{aligned} u_\omega &= \frac{u_r + u_l}{2} \\ u_\Psi &= u_r - u_l \end{aligned} \quad \Leftrightarrow \quad \begin{aligned} u_l &= u_\omega - \frac{u_\Psi}{2} \\ u_r &= u_\omega + \frac{u_\Psi}{2} \end{aligned}$$

## Task 2

## Task 3

In order to reach a conclusion about the stability of the angular displacement, it suffices to find a Lyapunov function $V(x)$ such that $V(0) = 0$, $V(x) > 0$ for all $x \neq 0$ and $\dot{V}(x) \leq 0$ for all x. Considering $x = \theta - \theta^G$ and $V(x) = x^2$:

$$V(0) = 0,\ V(x) > 0,\ \text{for all } x \neq 0, \text{ and}$$

$$\begin{aligned} \dot{V}(x) &= 2x\dot{x} = 2(\theta - \theta^G)\dot{\theta} \\ &= 2(\theta - \theta^G)\frac{R}{L}u_\Psi \end{aligned}$$

- When $\theta - \theta^G \leq 0$, $\dot{V}(x) = 2(\theta - \theta^G)\frac{R}{L} \leq 0$
- When $\theta - \theta^G > 0$, $\dot{V}(x) = -2(\theta - \theta^G)\frac{R}{L} < 0$

Hence $\dot{V}(x) \leq 0$ for all $x$, meaning that the system is stable for all $\theta \in (-180°, 180°]$.

## Task 4

Examining file `rot2.slx` one sees that $\dot{\theta} = R/Lu_\Psi$ is stable. We can verify this analytically:

$$
\begin{aligned}
\dot{u}_\Psi &= K_L(u_\Psi^R - u_\Psi) \\
\dot{u}_\Psi &= K_L u_\Psi^R - K_L u_\Psi \\
\dot{u}_\Psi \cdot e^{K_L t} &= K_L u_\Psi^R \cdot e^{K_L t} - K_L u_\Psi \cdot e^{K_L t} \\
\dot{u}_\Psi \cdot e^{K_L t} + K_L u_\Psi \cdot e^{K_L t} &= K_L u_\Psi^R \cdot e^{K_L t} \\
\frac{d}{dt}(u_\Psi e^{K_L t}) &= K_L u_\Psi^R e^{K_L t} \\
u_\Psi e^{K_L t} &= \int K_L u_\Psi^R e^{K_L t} = u_\Psi^R e^{K_L t} + \lambda \\
u_\Psi &= u_\Psi^R + \lambda e^{-K_L t}
\end{aligned}
$$

Hence

$$
u_\Psi(t) = \begin{cases} 1 + \lambda e^{-K_L t} & \theta - \theta^G \leq 0 \\ -1 + \lambda e^{-K_L t} & \theta - \theta^G > 0 \end{cases} \tag{1}
$$

where $u_\Psi(0) = u_\Psi^R(0) + \lambda \Leftrightarrow \lambda = u_\Psi(0) - u_\Psi^R(0)$.

In order to reach a conclusion about the stability of the angular displacement, it suffices to find a Lyapunov function $V(x)$ such that $V(0) = 0$, $V(x) > 0$ for all $x \neq 0$ and $\dot{V}(x) \leq 0$ for all x. Considering $x = \theta - \theta^G$ and $V(x) = x^2$:

$$
V(0) = 0, \; V(x) > 0, \text{ for all } x \neq 0, \text{ and}
$$

$$
\begin{aligned}
\dot{V}(x) &= 2x\dot{x} = 2(\theta - \theta^G)\dot{\theta} \\
&= 2(\theta - \theta^G)\frac{R}{L}u_\Psi \\
&= 2(\theta - \theta^G)\frac{R}{L}(u_\Psi^R + \lambda e^{-K_L t})
\end{aligned}
$$

- When $\theta - \theta^G \leq 0$, $\dot{V}(x) = 2(\theta - \theta^G)\frac{R}{L}(1 + \lambda e^{-K_L t}) \leq 0$
  With

$$
\begin{aligned}
&0 < e^{-K_L t} \leq 1 \\
&0 < \lambda e^{-K_L t} \leq \lambda, \text{ for } \lambda > 0 \\
&0 < 1 < 1 + \lambda e^{-K_L t} \leq 1 + \lambda, \text{ for } \lambda > 0
\end{aligned} \tag{2}
$$

- When $\theta - \theta^G > 0$, $\dot{V}(x) = 2(\theta - \theta^G)\frac{R}{L}(-1 + \lambda e^{-K_L t}) < 0$
  With

$$
\begin{aligned}
0 &< e^{-K_L t} \leq 1 \\
0 &< \lambda e^{-K_L t} \leq \lambda, \text{ for } \lambda > 0 \\
-1 &< -1 + \lambda e^{-K_L t} \leq -1 + \lambda < 0, \text{ for } \lambda > 0
\end{aligned} \tag{3}
$$

From inequalities 2 and 3 one gets

$$
\begin{aligned}
\lambda + 1 &> 0 \\
\lambda - 1 &< 0 \\
\lambda &> 0
\end{aligned}
$$

Hence $\dot{V}(x) \leq 0$ for all $x$ when $\lambda \in (0,1)$, meaning that the system is stable for all $\theta \in (-180°, 180°]$ and $\lambda \in (0,1)$.

# Task 5

# Task 6

# Task 7

$$
\begin{aligned}
\theta[k+1] &= \theta[k] + \frac{T_s R}{L} u_\Psi^R[k] \\
&= \theta[k] + \frac{T_s R}{L} K_\Psi^R (\theta^R - \theta[k]) \\
&= \theta[k](1 - \frac{T_s R}{L} K_\Psi^R) + \frac{T_s R}{L} K_\Psi^R \theta^R
\end{aligned}
$$

By subtracting $\theta^R$ from both sides one gets

$$
\begin{aligned}
\theta[k+1] - \theta^R &= \theta[k](1 - \frac{T_s R}{L} K_\Psi^R) + (\frac{T_s R}{L} K_\Psi^R - 1)\theta^R \\
&= (\theta[k] - \theta^R)(1 - \frac{T_s R}{L} K_\Psi^R) \qquad (4)
\end{aligned}
$$

We now define state $\theta'$ as

$$
\theta'[k] = \theta[k] - \theta^R
$$

Then, equation 4 becomes

$$
\theta'[k+1] = \theta'[k](1 - \frac{T_s R}{L} K_\Psi^R)
$$

In order for this system to be stable, that is, $|\theta - \theta^R| \to 0$ as $k \to \infty$, the solution of the equation inside the parentheses should lie inside the unit circle:

$$\begin{aligned}
\left|1 - \frac{T_s R}{L} K_{\Psi}^{R}\right| &< 1 \\
-1 < 1 - \frac{T_s R}{L} K_{\Psi}^{R} &< 1 \\
-2 < -\frac{T_s R}{L} K_{\Psi}^{R} &< 0 \\
0 < \frac{T_s R}{L} K_{\Psi}^{R} &< 2 \\
0 < K_{\Psi}^{R} &< \frac{2L}{T_s R}
\end{aligned} \tag{5}$$

Hence, the maximum value $K_{\Psi}^{R}$ can take for the system to be marginally stable is $K_{\Psi,max}^{R} = \dfrac{2L}{T_s R}$

Theoretically, the value of $K_{\Psi}^{R}$ can be chosen to be any value inside the interval defined in inequality 5. However, first, it would be wise to choose a value that is far enough from the maximum value so as to avoid overshoot, but close enough to it, so that convergence happens in reasonable time. Hence, in practice, it is reasonable that one would need to experiment with different values and choose one that results in balancing a small angular error, a minimal overshoot, if any, and a quick enough settling time.

Eventually, the choice made for $K_{\Psi}^{R}$ was $K_{\Psi}^{R} = \frac{1}{2} K_{\Psi,max}^{R}$.

# Task 8

For the purpose of simulating this part of the controller, the initial point of the robot was taken to be $I(x_0, y_0) \equiv (0, 0)$. The goal was set to $G(x_g, y_g) \equiv (-0.37, 1.68)$, which is node 1 in the simulation environment. The angle between the line connecting $I$ and $G$ and the x-axis is hence $\theta_R = tan^{-1}(1.68/-0.37) = 102.42$ degrees.

Figures 2, 4, 6, 8, 10 show the angular response of the robot for different values of $K_{\Psi}^{R}$ inside the interval set by inequality 5. Figure 12 verifies that the upper limit for $K_{\Psi}^{R}$ is indeed $K_{\Psi,max}^{R} = \frac{2L}{T_s R}$ by showing that the angular response of the robot cannot converge for $K_{\Psi}^{R} > K_{\Psi,max}^{R}$.

Here, one can see that the smaller the value of $K_{\Psi}^{R}$ is, the larger the settling time, the lower the rise time and the smoother the response is. However, as the value of $K_{\Psi}^{R}$ increases, the steady-state response begins to oscillate, with the amplitude of this oscillation proportional to the value of $K_{\Psi}^{R}$.

Figures 3, 5, 7, 9 and 3 focus on the steady-state value of the aforementioned responses. As it is evident, none of the responses converge to the value $\theta_R = 102.42$. This is reasonable since with only a purely proportional control signal, as the angular error, i.e. $e(\theta) = \theta^R - \theta$, tends to zero, the product of $K_{\Psi}^{R}$ and $e(\theta)$ isn't large enough to force the robot to rotate exactly $\theta^R$ degrees.

Another way to look at this is by looking at the steady-state response of the system, which is linear, for a step input of magnitude $\theta^R$. Figure 1 shows the structure of the system. The z-transform of the input is then $R(z) = \dfrac{\theta^R}{1 - z^{-1}}$ and the equation of the closed-loop system is

$$Y(z) = \frac{K_{\Psi}^{R} G(z)}{1 + K_{\Psi}^{R} G(z)} R(z)$$

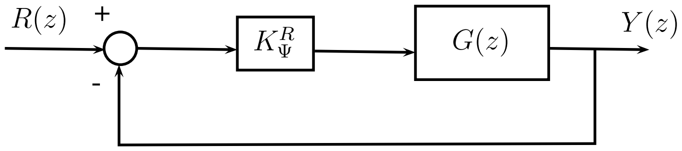


Figure 1: The structure of the system under rotational control. $G(z)$ is the discretized transfer function of the linear system whose state-space equation is $\dot{\theta} = \frac{R}{L}u_\Psi$

The steady-state response is

$$lim_{t\to\infty}y(t) = lim_{z\to 1}(1-z^{-1})\frac{\theta^R}{1-z^{-1}}\frac{K_\Psi^R G(z)}{1+K_\Psi^R G(z)} = \theta^R \cdot lim_{z\to 1}\frac{K_\Psi^R G(z)}{1+K_\Psi^R G(z)}$$

The steady-state response cannot reach exactly $\theta^R$ as the above limit cannot converge to 1 under our limitations for $K_\Psi^R$ and the dynamics of $G(z)$.

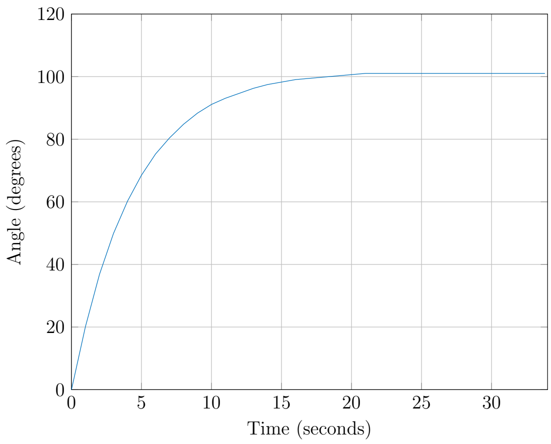


Figure 2: The orientation of the robot over time for $K_\Psi^R = 0.1K_{\Psi,max}^R$

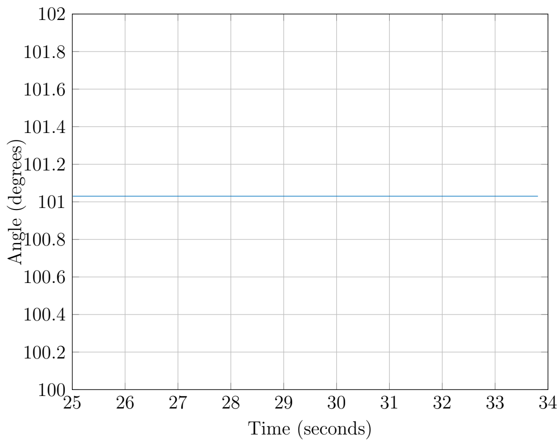


Figure 3: The steady state orientation of the robot for $K_\Psi^R = 0.1K_{\Psi,max}^R$

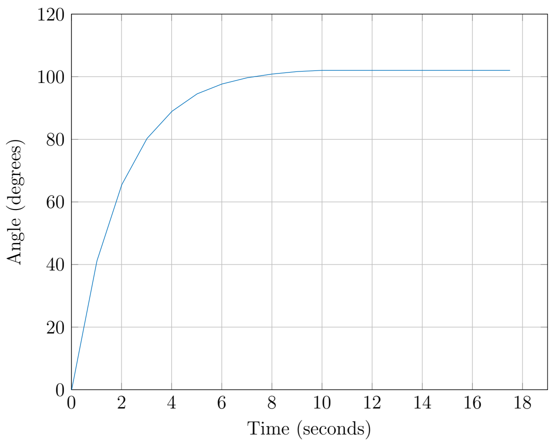


Figure 4: The orientation of the robot over time for $K_\Psi^R = 0.2K_{\Psi,max}^R$

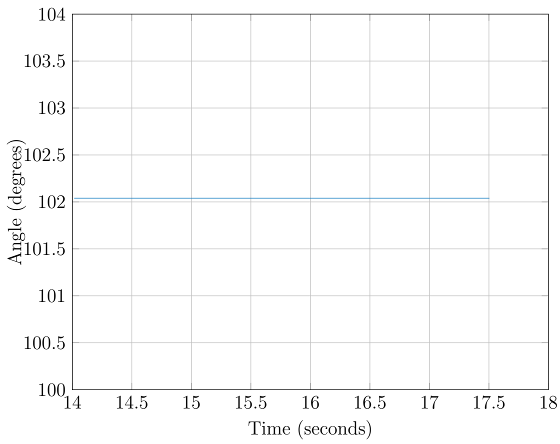


Figure 5: The steady state orientation of the robot for $K_\Psi^R = 0.2K_{\Psi,max}^R$

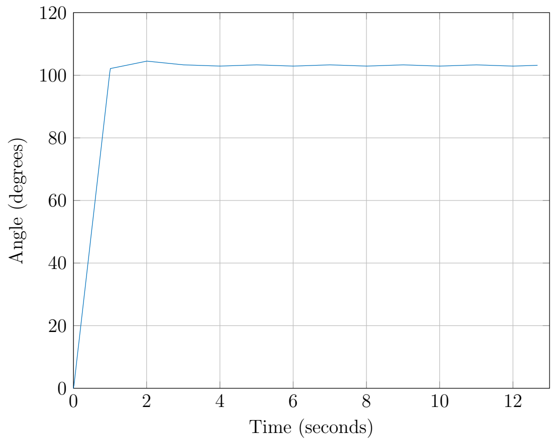


Figure 6: The orientation of the robot over time for $K_{\Psi}^{R} = 0.5K_{\Psi,max}^{R}$

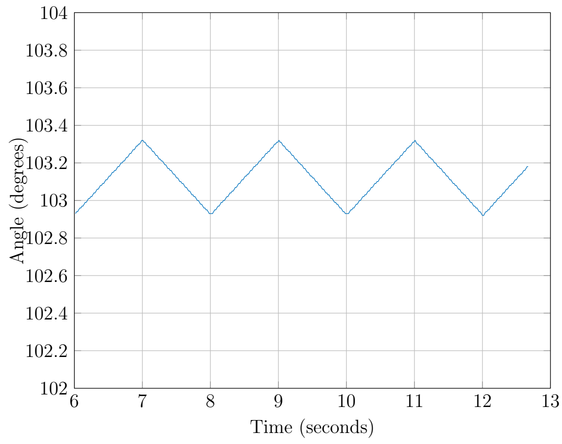


Figure 7: The steady state orientation of the robot for $K_{\Psi}^{R} = 0.5K_{\Psi,max}^{R}$

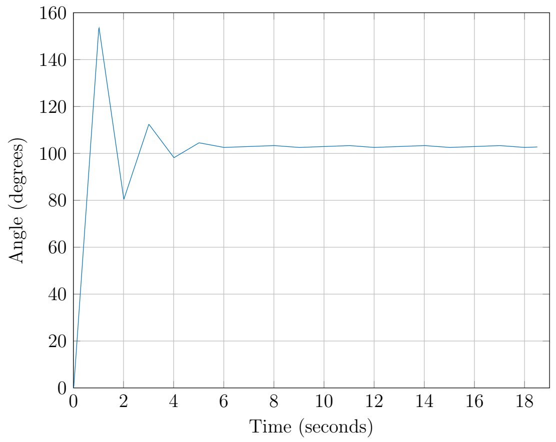


Figure 8: The orientation of the robot over time for $K_{\Psi}^{R} = 0.75K_{\Psi,max}^{R}$

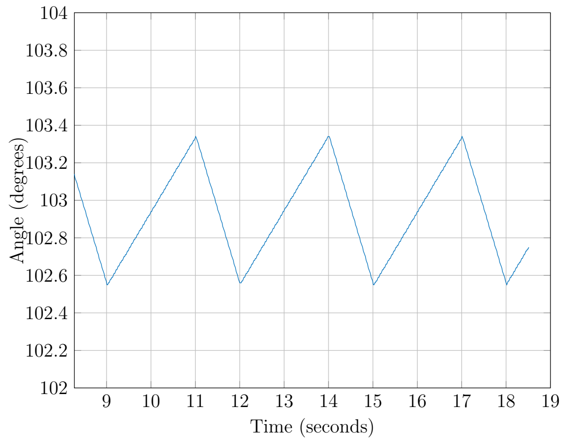


Figure 9: The steady state orientation of the robot for $K_{\Psi}^{R} = 0.75K_{\Psi,max}^{R}$

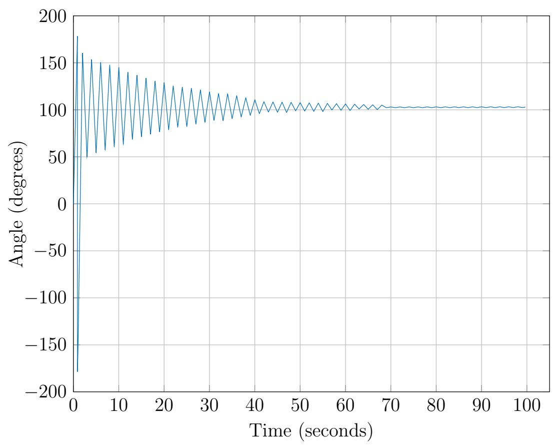


Figure 10: The orientation of the robot over time for $K_{\Psi}^{R} = K_{\Psi,max}^{R}$. This is the upper limit value of $K_{\Psi}^{R}$ before the system becomes unstable

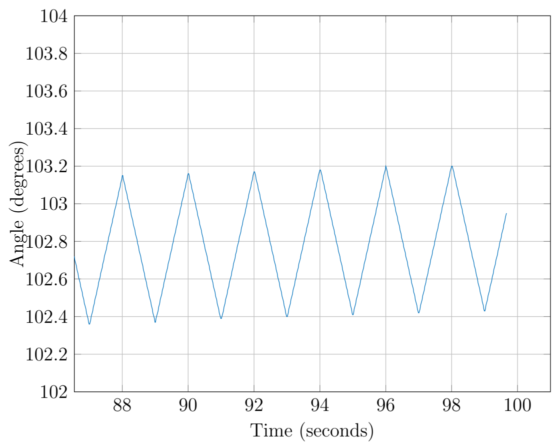


Figure 11: The steady state orientation of the robot for $K_{\Psi}^{R} = K_{\Psi,max}^{R}$

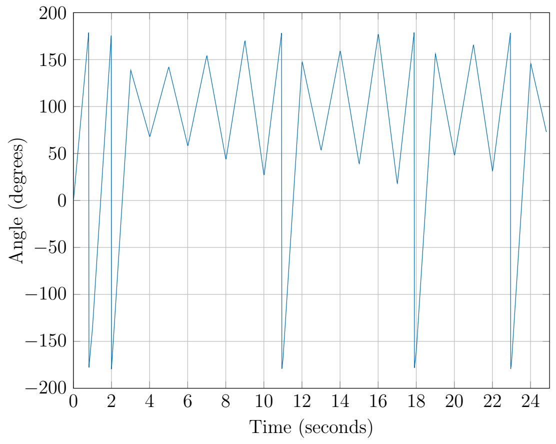


Figure 12: The orientation of the robot over time for $K^R_\Psi = K^R_{\Psi,max} + 1$. The system is indeed unstable

# Task 9

$$
\begin{aligned}
d_0[k] &= cos(\theta[k])(x_0 - x[k]) + sin(\theta[k])(y_0 - y[k]) \\
&= cos(\theta[k])(x_0 - x[k-1] - T_s R u^R_\omega[k-1] cos(\theta[k-1])) \\
&+ sin(\theta[k])(y_0 - y[k-1] - T_s R u^R_\omega[k-1] sin(\theta[k-1])) \\
&= cos(\theta^R)(x_0 - x[k-1] - T_s R u^R_\omega[k-1] cos(\theta^R)) \\
&+ sin(\theta^R)(y_0 - y[k-1] - T_s R u^R_\omega[k-1] sin(\theta^R)) \\
&= cos(\theta^R)(x_0 - x[k-1]) + sin(\theta^R)(y_0 - y[k-1]) - T_s R K^T_\omega d_0[k-1] \\
&= d_0[k-1] - T_s R K^T_\omega d_0[k-1] \\
&= (1 - T_s R K^R_\omega) d_0[k-1]
\end{aligned}
$$

Hence

$$d_0[k+1] = (1 - T_s R K^R_\omega) d_0[k]$$

In order for this system to be stable, that is, $d_0 \to 0$ as $k \to \infty$, the solution of the equation inside the parentheses should lie inside the unit circle:

$$
\begin{aligned}
\left|1 - T_s R K^R_\omega\right| &< 1 \\
-1 < 1 - T_s R K^R_\omega &< 1 \\
-2 < -T_s R K^R_\omega &< 0 \\
0 < T_s R K^R_\omega &< 2 \\
0 < K^R_\omega &< \frac{2}{T_s R}
\end{aligned}
\tag{6}
$$

Hence, the maximum value $K_\omega^R$ can take for the system to be marginally stable is $K_{\omega,max}^R = \dfrac{2}{T_s R}$.

Theoretically, the value of $K_\omega^R$ can be chosen to be any value inside the interval defined in inequality 6. However, first, it would be wise to choose a value that is far enough from the maximum value so as to avoid overshoot, but close enough to it, so that convergence happens in reasonable time. Hence, in practice, it is reasonable that one would need to experiment with different values and choose one that results in balancing a small angular error, a minimal overshoot, if any, and a quick enough settling time.

Eventually, the choice made for $K_\omega^R$ was $K_\omega^R = \frac{1}{2} K_{\omega,max}^R$.

# Task 10

This part of the controller is responsible for compensating translational errors during rotation. Since the rotational speed $u_\Psi$ is zero, it is expected that the robot will not move away from its origin. Figure 13 plots the robot's distance from its origin over time for $K_\omega^R = 0.5 K_{\omega,max}^R$.

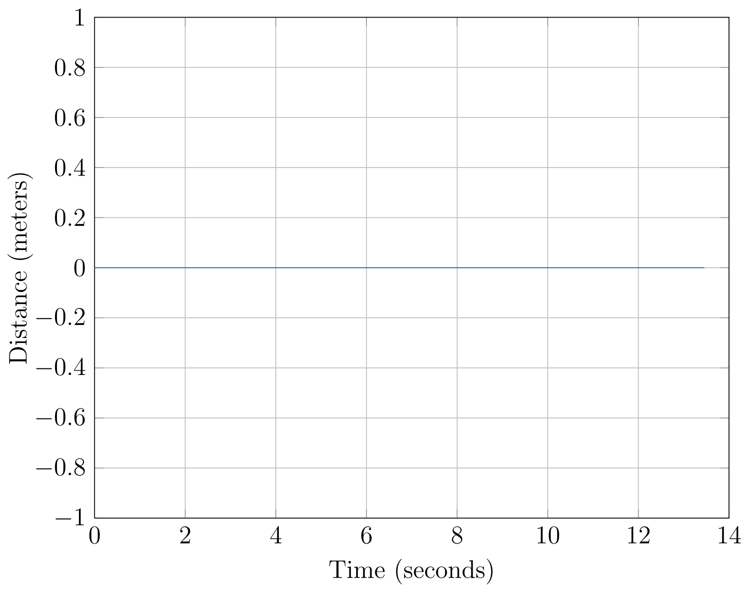


Figure 13: The distance of the robot from its origin position over time for $K_\omega^R = 0.5 K_{\omega,max}^R$

# Task 11

Figures 14, 16, 18, 20, 22 show the bearing error of the robot for different values of $K_\Psi^R$ inside the interval set by inequality 5. Figures 15, 17, 19, 21 and 15 focus on the steady-state bearing error. Figure 24 illustrates the $d_0[k]$ error, which is at all times zero.

The evolution of the bearing and distance error is the same when both of the rotational controllers are enabled compared to when only one of them is enabled. This happens because the behaviour of each controller does not affect the behaviour of the other, since this is an ideal system. In reality, we expect that the distance error will be non-zero.

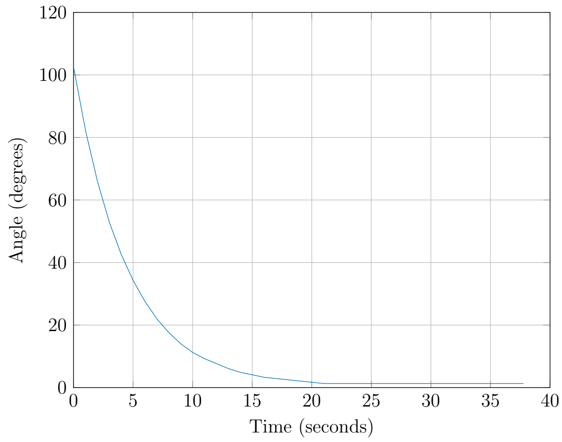


Figure 14: The error in orientation of the robot over time for $K^R_\Psi = 0.1 K^R_{\Psi,max}$

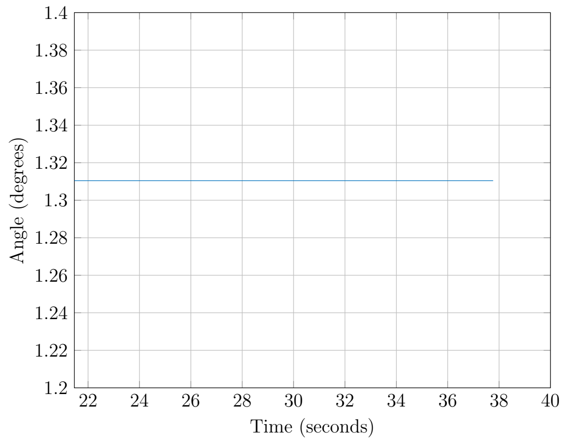


Figure 15: The steady state error in orientation of the robot for $K^R_\Psi = 0.1 K^R_{\Psi,max}$

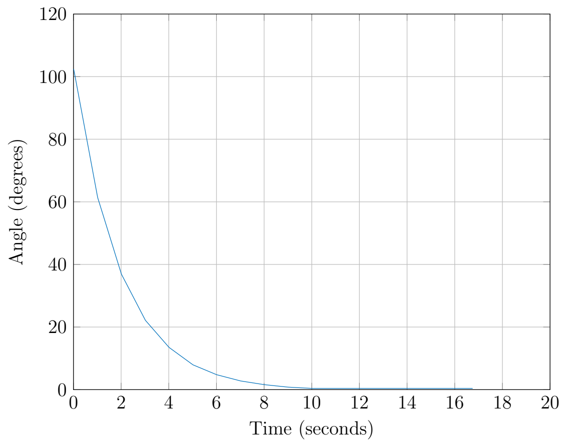


Figure 16: The error in orientation of the robot over time for $K^R_\Psi = 0.2 K^R_{\Psi,max}$

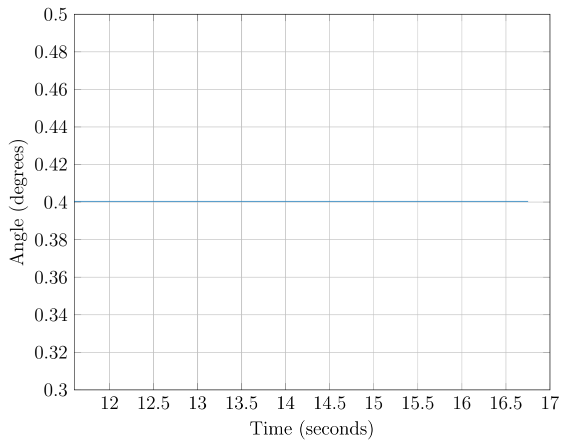


Figure 17: The steady state error in orientation of the robot for $K^R_\Psi = 0.2 K^R_{\Psi,max}$

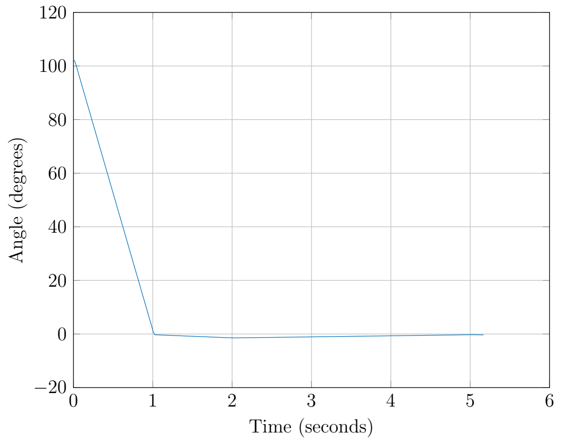


Figure 18: The error in orientation of the robot over time for $K^R_\Psi = 0.5K^R_{\Psi,max}$

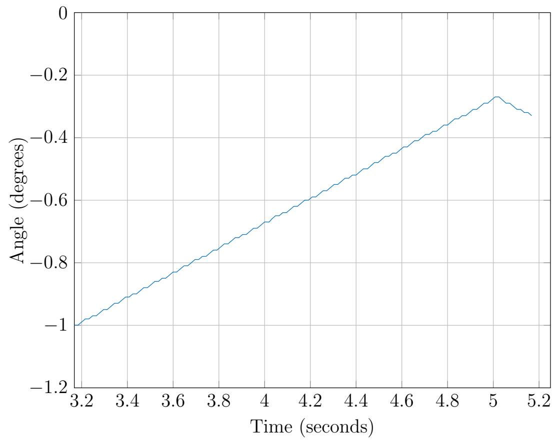


Figure 19: The steady state error in orientation of the robot for $K^R_\Psi = 0.5K^R_{\Psi,max}$

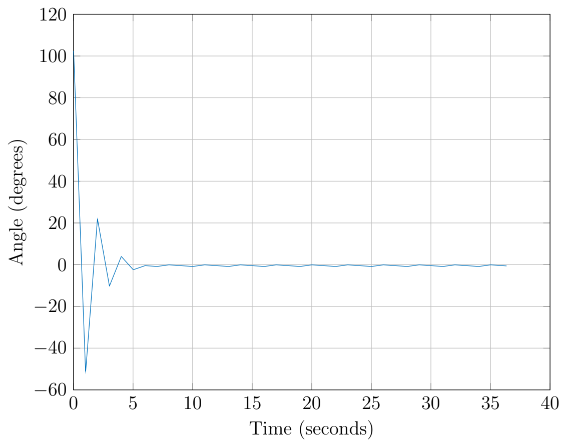


Figure 20: The error in orientation of the robot over time for $K^R_\Psi = 0.75K^R_{\Psi,max}$

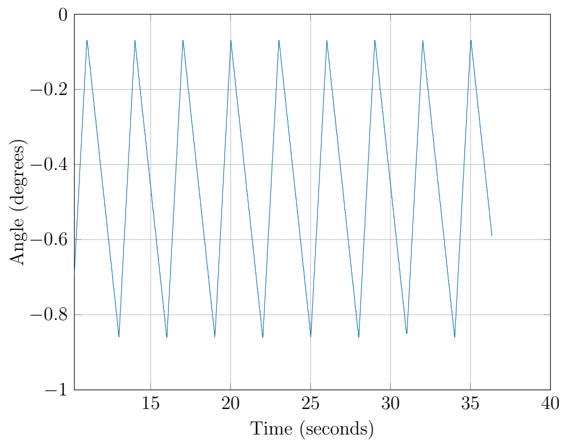


Figure 21: The steady state error in orientation of the robot for $K^R_\Psi = 0.75K^R_{\Psi,max}$

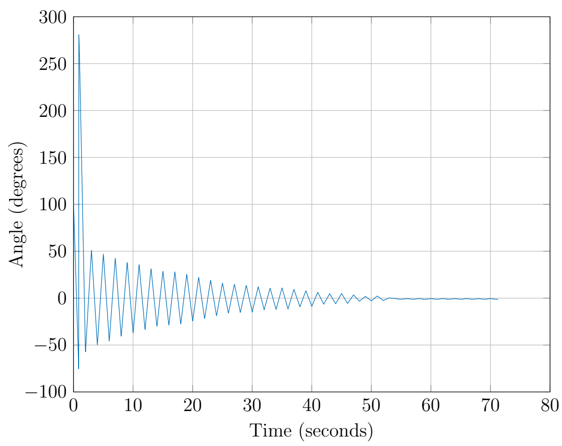


Figure 22: The error in orientation of the robot over time for $K^R_\Psi = K^R_{\Psi,max}$.

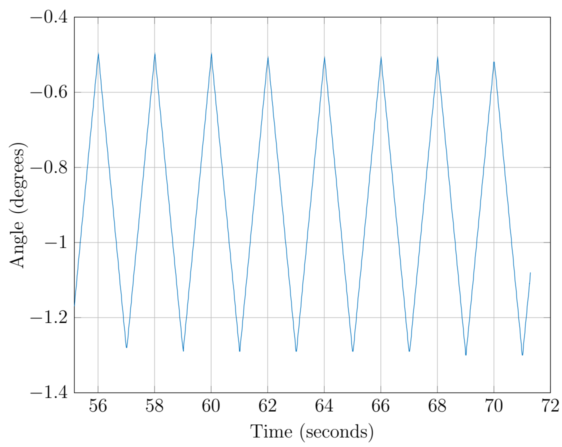


Figure 23: The steady state error in orientation of the robot for $K^R_\Psi = K^R_{\Psi,max}$

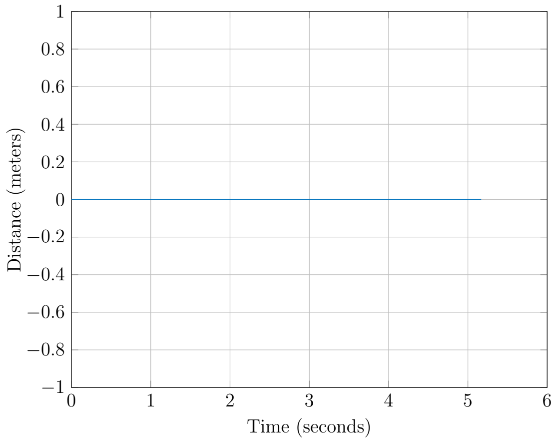


Figure 24: The distance of the robot from its origin position over time for all legitimate values or $K_\omega^R$

# Task 12

$$\begin{aligned} d_g[k] &= cos(\theta_g)(x_g - x[k]) + sin(\theta_g)(y_g - y[k]) \\ &= cos(\theta_g)(x_g - x[k-1] - T_s R u_\omega^T[k-1] cos(\theta_g)) + \\ & sin(\theta_g)(y_g - y[k-1] - T_s R u_\omega^T[k-1] sin(\theta_g)) \\ &= cos(\theta_g)(x_g - x[k-1]) + sin(\theta_g)(y_g - y[k-1]) - T_s R K_\omega^T d_g[k-1] \\ &= d_g[k-1] - T_s R K_\omega^T d_g[k-1] \\ &= (1 - T_s R K_\omega^T) d_g[k-1] \end{aligned}$$

Hence

$$d_g[k+1] = (1 - T_s R K_\omega^T) d_g[k]$$

In order for this system to be stable, that is, $d_g \to 0$ as $k \to \infty$, the solution of the equation inside the parentheses should lie inside the unit circle:

$$\begin{aligned} \left|1 - T_s R K_\omega^T\right| &< 1 \\ -1 < 1 - T_s R K_\omega^T &< 1 \\ -2 < -T_s R K_\omega^T &< 0 \\ 0 < T_s R K_\omega^T &< 2 \\ 0 < K_\omega^T &< \frac{2}{T_s R} \end{aligned} \tag{7}$$

Hence, the maximum value $K_\omega^T$ can take for the system to be marginally stable is $K_{\omega,max}^T = \dfrac{2}{T_s R}$

Theoretically, the value of $K_\omega^T$ can be chosen to be any value inside the interval defined in inequality 7. However, first, it would be wise to choose a value that is far enough from the maximum value so as to avoid overshoot, but close enough to it, so that convergence happens in reasonable time. Hence, in practice, it is reasonable that one would need to experiment with different values and choose one that results in balancing a small angular error, a minimal overshoot, if any, and a quick enough settling time.

Eventually, the choice made for $K_\omega^T$ was $K_\omega^T = \frac{1}{2} K_{\omega,max}^T$.

# Task 13

For the purpose of simulating this part of the controller, the initial point of the robot was taken to be $I(x_0, y_0) \equiv (0, 0)$. The goal was set to $G(x_g, y_g) \equiv (1.0, 0.0)$.

Figures 25, 27, 29, 31 and 33 show the displacemental response of the robot for various values of $K_\omega^T$ inside the interval set by inequality 7. Figure 35 verifies that the upper limit for $K_\omega^T$ is indeed $\frac{2}{T_s R}$ by showing that the displacemental response of the robot cannot converge for $K_\omega^T > K_{\omega,max}^T$.

Here, one can see that the smaller the value of $K_\omega^T$ is, the larger the settling time, the lower the rise time and the smoother the response is. However, as the value of $K_\omega^T$ increases, the steady-state response begins to oscillate, with the amplitude of this oscillation proportional to the value of $K_\omega^T$.

Figures 26, 28, 30, 32 and 34 focus on the steady-state value of the aforementioned responses. In contrast to the proportional rotational controller, the robot *can* arrive to its reference signal. The equations that govern the robot's translational movement are non-linear, as opposed to the one that governs its rotational movement, which in turn means that the translational system's behaviour is not bounded within the laws that govern control with proportional controllers on linear systems.

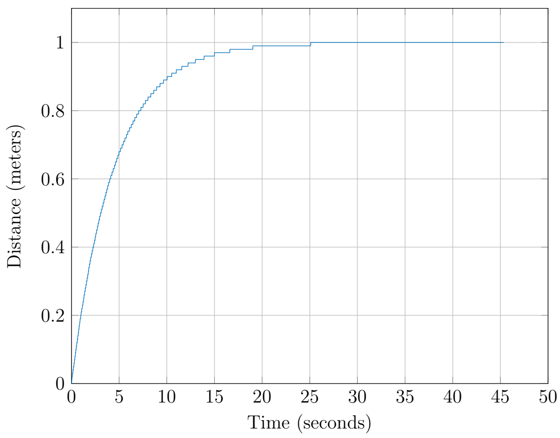


Figure 25: The orientation of the robot over time for $K_\omega^T = 0.1 K_{\omega,max}^T$

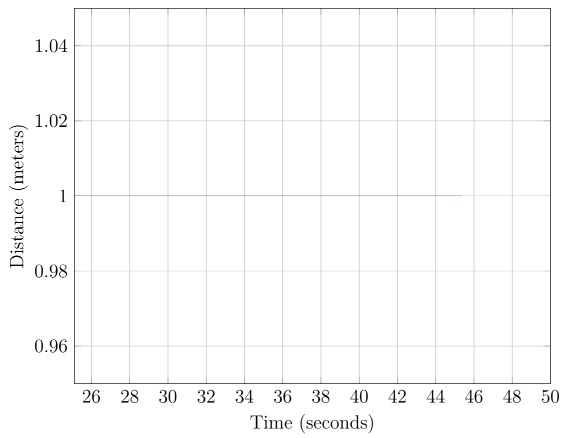


Figure 26: The steady state orientation of the robot for $K_\omega^T = 0.1 K_{\omega,max}^T$

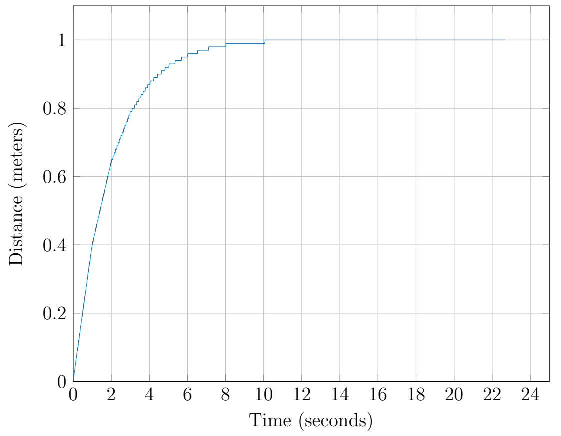


Figure 27: The orientation of the robot over time for $K^T_\omega = 0.2K^T_{\omega,max}$

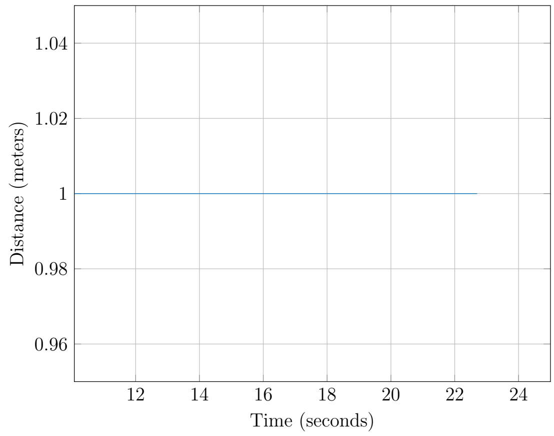


Figure 28: The steady state orientation of the robot for $K^T_\omega = 0.2K^T_{\omega,max}$

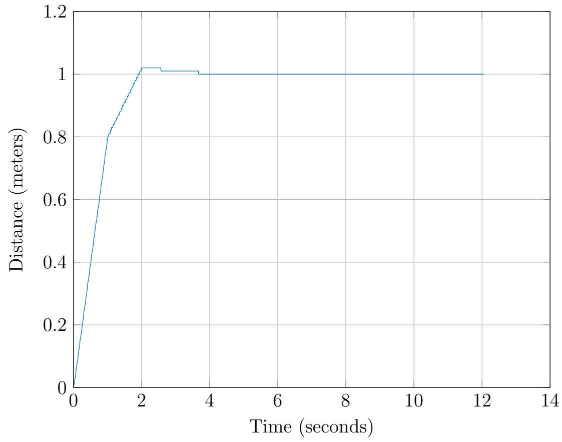


Figure 29: The orientation of the robot over time for $K^T_\omega = 0.5K^T_{\omega,max}$

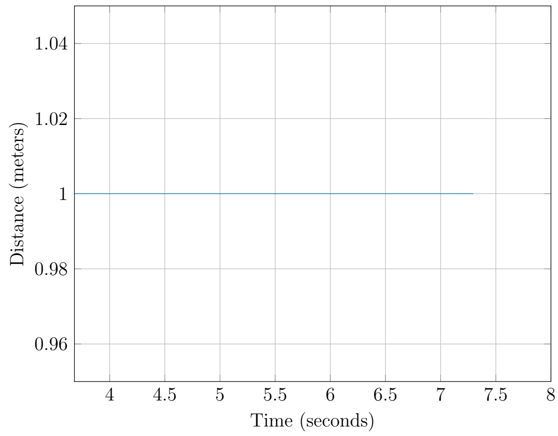


Figure 30: The steady state orientation of the robot for $K^T_\omega = 0.5K^T_{\omega,max}$

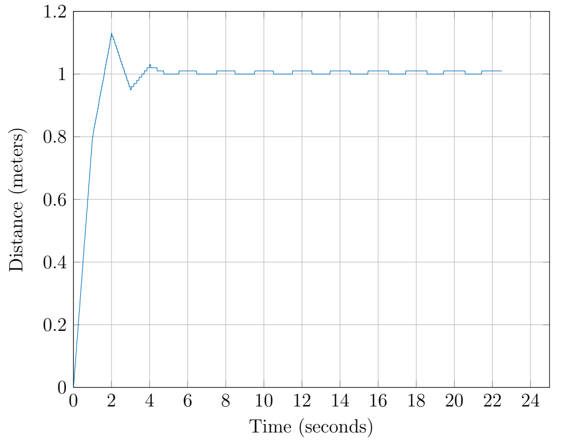


Figure 31: The orientation of the robot over time for $K^T_\omega = 0.75K^T_{\omega,max}$

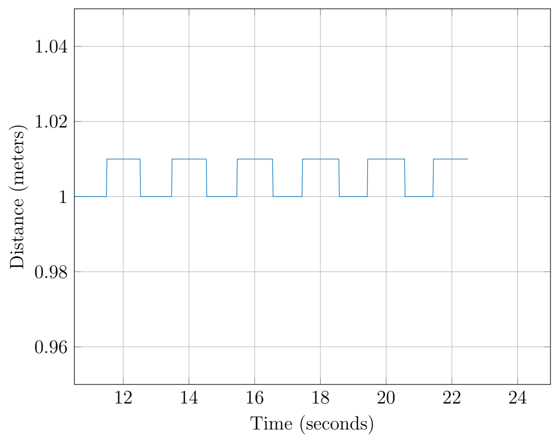


Figure 32: The steady state orientation of the robot for $K^T_\omega = 0.75K^T_{\omega,max}$

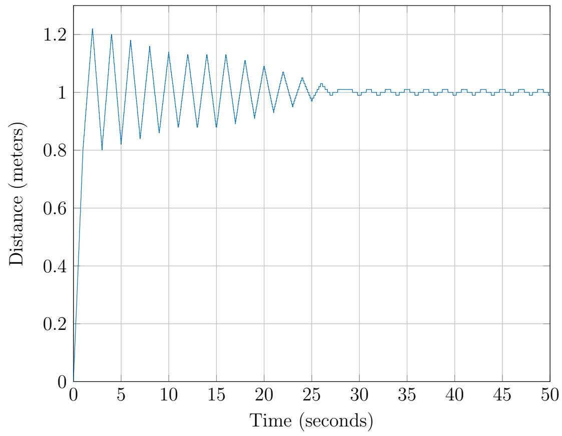


Figure 33: The orientation of the robot over time for $K_\omega^T = K_{\omega,max}^T$.

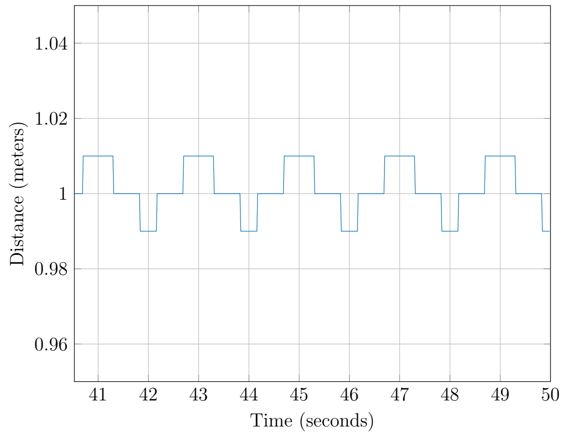


Figure 34: The steady state orientation of the robot for $K_\omega^T = K_{\omega,max}^T$

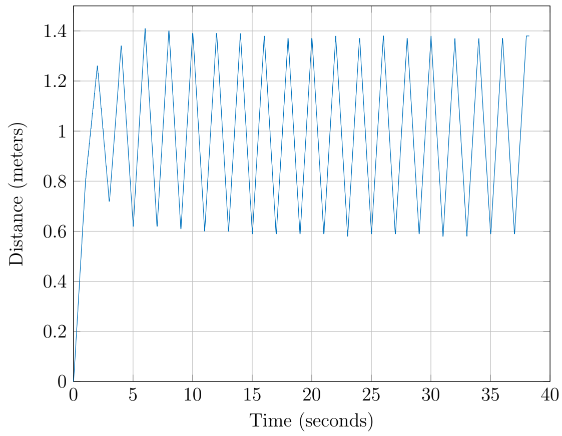


Figure 35: The orientation of the robot over time for $K_\omega^T = 1.1K_{\omega,max}^T$. The system is marginally stable

# Task 14

$$d_p[k+1] = p(\theta[k+1] - \theta_g) \tag{8}$$

But

$$\theta[k+1] = \theta[k] + T_s \frac{R}{L} u_\Psi^T[k]$$

Hence equation 8 becomes

$$
\begin{aligned}
d_p[k+1] &= p(\theta[k] + T_s\frac{R}{L}u_{\Psi}^T[k] - \theta_g) \\
&= p(\theta[k] + T_s\frac{R}{L}K_{\Psi}^T d_p[k] - \theta_g) \\
&= pT_s\frac{R}{L}K_{\Psi}^T d_p[k] + p(\theta[k] - \theta_g) \\
&= pT_s\frac{R}{L}K_{\Psi}^T d_p[k] + d_p[k] \\
&= d_p[k](1 + pT_s\frac{R}{L}K_{\Psi}^T d_p[k])
\end{aligned}
$$

In order for this system to be stable, that is, $d_p \to 0$ as $k \to \infty$, the solution of the equation inside the parentheses should lie inside the unit circle:

$$
\begin{aligned}
\left|1+pT_sRK_{\omega}^T\right| &< 1 \\
-1 < 1+pT_sRK_{\omega}^T &< 1 \\
-2 < pT_sRK_{\omega}^T &< 0 \\
-\frac{2}{pT_sR} < K_{\omega}^T &< 0
\end{aligned}
\tag{9}
$$

Hence, the maximum value $K_{\omega}^T$ can take for the system to be marginally stable is $K_{\omega,max}^T = 0$.

Theoretically, the value of $K_{\omega}^T$ can be chosen to be any value inside the interval defined in inequality 6. However, first, it would be wise to choose a value that is far enough from the maximum value so as to avoid overshoot, but close enough to it, so that convergence happens in reasonable time. Hence, in practice, it is reasonable that one would need to experiment with different values and choose one that results in balancing a small angular error, a minimal overshoot, if any, and a quick enough settling time.

Eventually, the choice made for $K_{\omega}^T$ was $K_{\omega}^T = \frac{1}{2}K_{\omega,min}^T = -\frac{1}{pT_sR}$.

# Task 15

Inequality 9 tells us that the higher the value of $p$, the broader the region of values for $K_{\Psi}^T$ is so that the systems is stable. Hence, the lower the value of $p$ is, the worse the robot's ability to follow a line is.

# Task 16

This part of the controller is responsible for compensating for rotational errors during translation. Since the translational velocity $u_{\omega}$ is zero, it is expected that the robot will not rotate away from its original bearing. Figure 36 plots the robot's bearing with regard to its original bearing of 0 degrees over time for $K_{\Psi}^T = 0.5K_{\Psi,min}^T$.

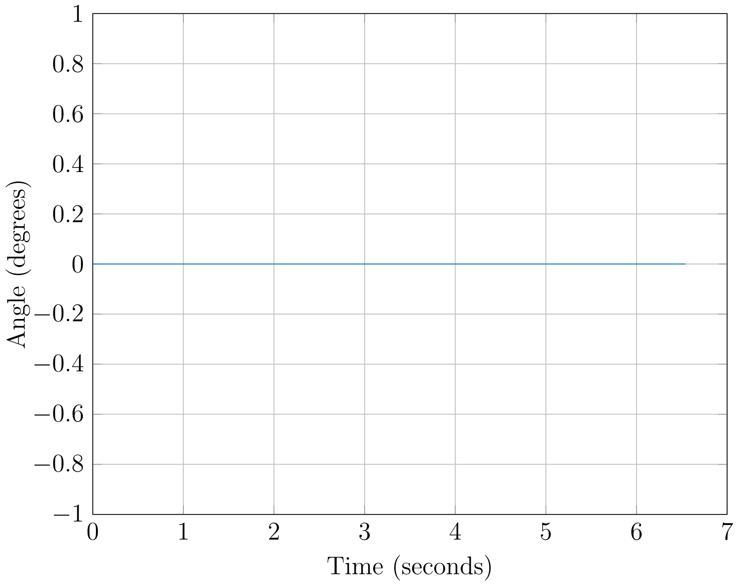


Figure 36: The angular displacement of the robot from its original bearing over time for $K_{\Psi}^{T} = 0.5K_{\Psi,min}^{T}$

# Task 17

Figures 37, 39, 41, 43 and show the displacemental error of the robot for different values of $K_{\omega}^{T}$ inside the interval set by inequality 9. Figures 38, 40, 42 and 44 focus on the steady-state displacemental error. Figure 45 illustrates the $d_0[k]$ error, which is at all times zero.

The evolution of the bearing and displacement error is the same when both of the translational controllers are enabled compared to when only one of them is enabled. This happens because the behaviour of each controller does not affect the behaviour of the other, since this is an ideal system. In reality, we expect that the angular error will be non-zero.

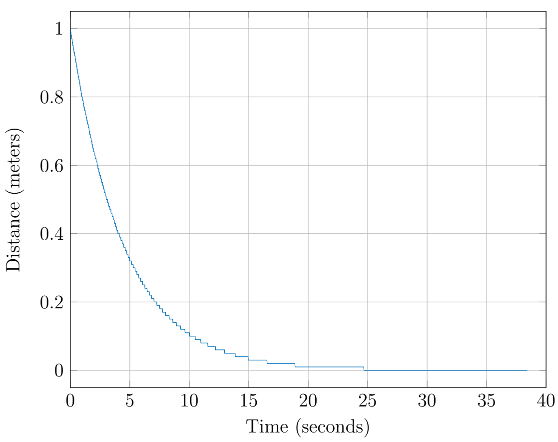


Figure 37: The error in displacement of the robot over time for $K_{\omega}^{T} = 0.1K_{\omega,max}^{T}$

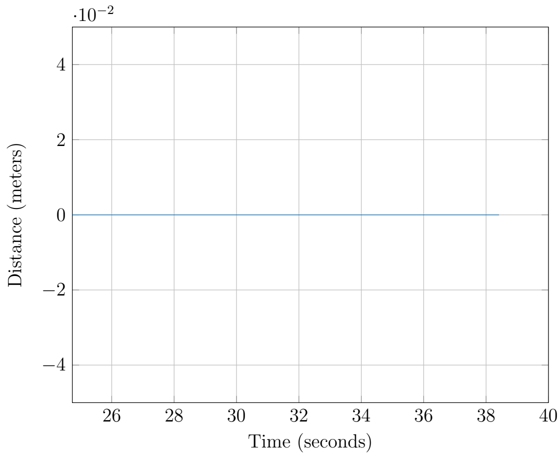


Figure 38: The steady state error in displacement of the robot for $K_{\omega}^{T} = 0.1K_{\omega,max}^{T}$

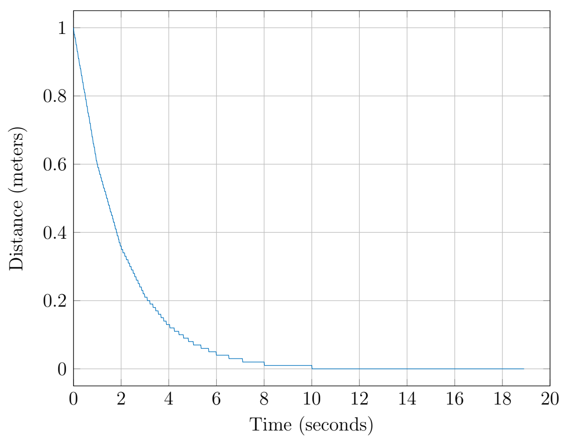


Figure 39: The error in displacement of the robot over time for $K_{\omega}^{T} = 0.2K_{\omega,max}^{T}$

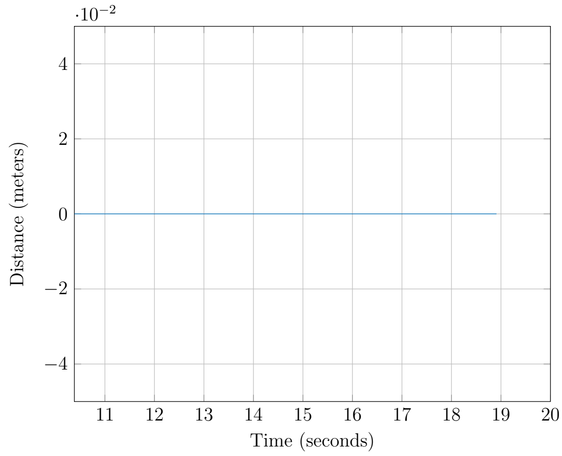


Figure 40: The steady state error in displacement of the robot for $K_{\omega}^{T} = 0.2K_{\omega,max}^{T}$

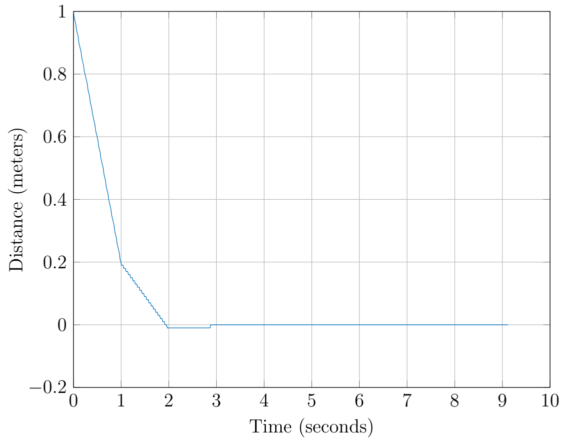


Figure 41: The error in displacement of the robot over time for $K_{\omega}^{T} = 0.5K_{\omega,max}^{T}$

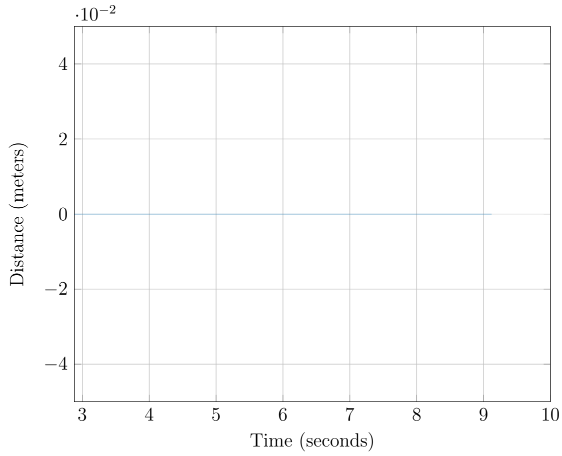


Figure 42: The steady state error in displacement of the robot for $K_{\omega}^{T} = 0.5K_{\omega,max}^{T}$

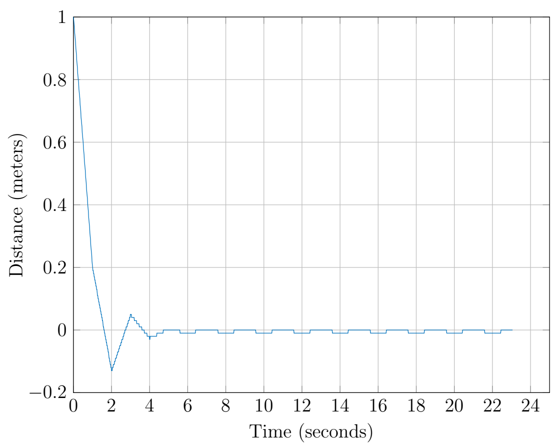


Figure 43: The error in displacement of the robot over time for $K_\omega^T = 0.75 K_{\omega,max}^T$

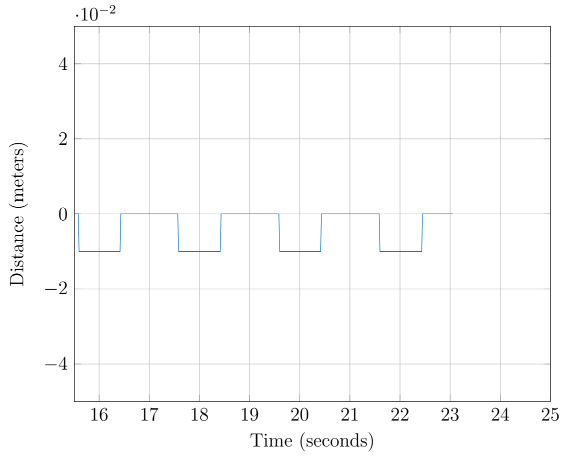


Figure 44: The steady state error in displacement of the robot for $K_\omega^T = 0.75 K_{\omega,max}^T$

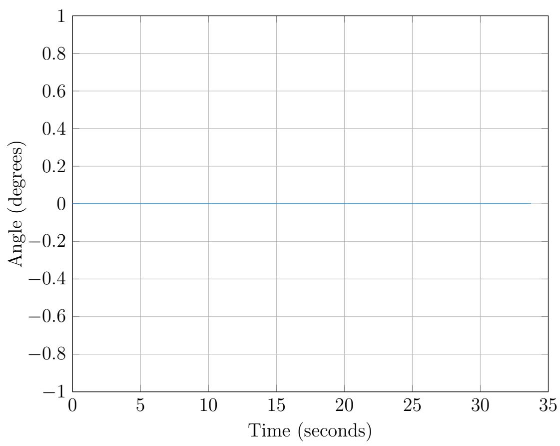


Figure 45: The steady state error in orientation of the robot for all legitimate values of $K_\omega^T$

# Task 18

# Task 19

Evaluating the performance of the hybrid automaton primarily involves the evaluation of the steady-state errors regarding the position and angle of the robot with regard to the selected goal position. In order to obtain a broader understanging of how the four $K_*$ gains influence the trajectory of the robot, twelve combinations were considered for the 4-tuple

$$(K_\Psi^R, K_\omega^R, K_\Psi^T, K_\omega^T)$$

where

$$K_\Psi^R \in \{0.1, 0.2, 0.5\} \cdot K_{\Psi,max}^R$$

$$K_\omega^T \in \{0.1, 0.2, 0.5, 0.75\} \cdot K_{\omega,max}^T$$

$$K_\omega^R = 0.5K^R_{\omega,max}, \text{ and } K_\Psi^T = 0.5K^T_{\Psi,max}$$

Figures 46 - ?? on the left-hand side illustrate the evolution of the distance of the robot in relation to its goal, while figures on the right-hand side display the evolution of the angular error over time. The goal was set to be node 1 $N1(-0.37, 1.68)$, and the robot's initial pose was $(x_0, y_0, \theta_0) \equiv (0, 0, 0)$. Hence, the distance to the goal was $d_g = 1.7203$ meters and the angle to the goal $\theta^R = 102.42°$. The distance and angle tolerance thresholds where taken to be $d_{th} = 2$ cm and $\theta_{th} = 2°$ respectively.

Since the actual final pose is not defined deterministically, five simulations of each possible combination of settings for the aforementioned 4-tuple were conducted. Hence, all the following figures express the mean steady-state positional and angular errors across five runs.

Table ?? illustrates the steady-state errors $e_d$ and $e_\theta$ regarding the distance and the angle that the robot had to travel, respectively.

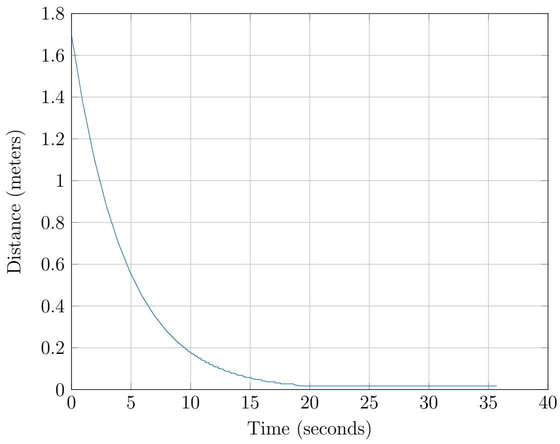


Figure 46: The error in displacement of the robot over time for $(K^R_\Psi, K^T_\omega) \equiv (0.1K^R_{\Psi,max}, 0.1K^T_{\omega,max})$

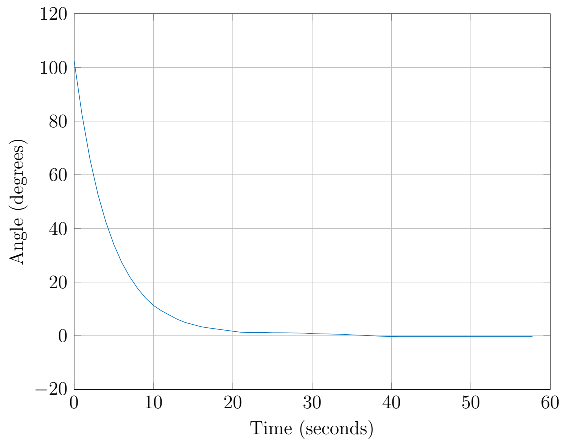


Figure 47: The error in bearing of the robot over time for $(K^R_\Psi, K^T_\omega) \equiv (0.1K^R_{\Psi,max}, 0.1K^T_{\omega,max})$

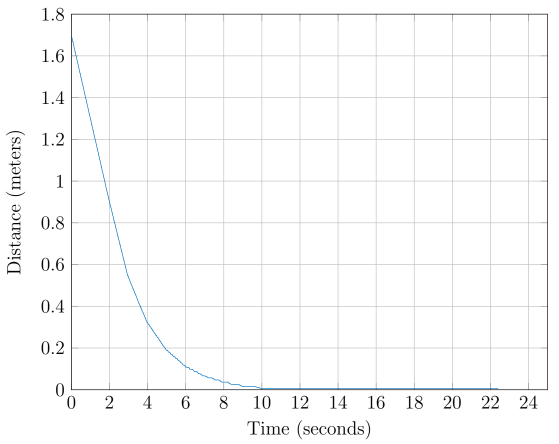


Figure 48: The error in displacement of the robot over time for $(K^R_\Psi, K^T_\omega) \equiv (0.1K^R_{\Psi,max}, 0.2K^T_{\omega,max})$

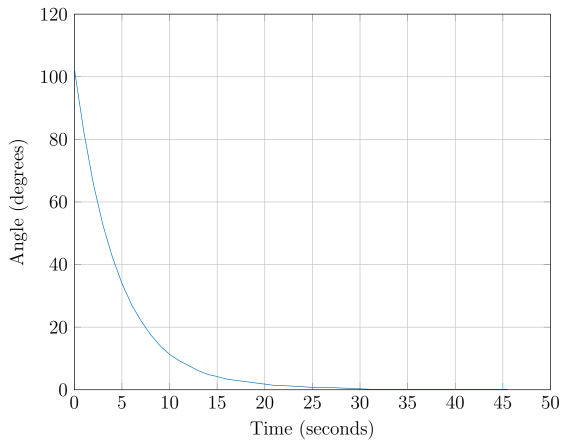


Figure 49: The error in bearing of the robot over time for $(K^R_\Psi, K^T_\omega) \equiv (0.1K^R_{\Psi,max}, 0.2K^T_{\omega,max})$

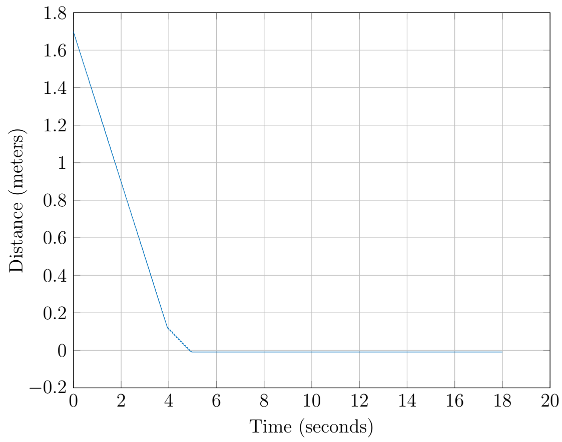


Figure 50: The error in displacement of the robot over time for $(K^R_\Psi, K^T_\omega) \equiv (0.1K^R_{\Psi,max}, 0.5K^T_{\omega,max})$

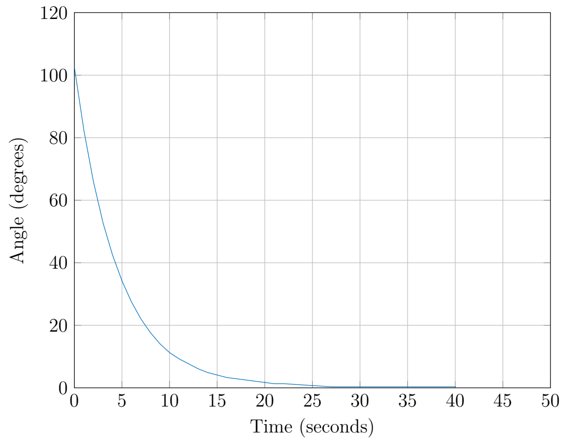


Figure 51: The error in bearing of the robot over time for $(K^R_\Psi, K^T_\omega) \equiv (0.1K^R_{\Psi,max}, 0.5K^T_{\omega,max})$

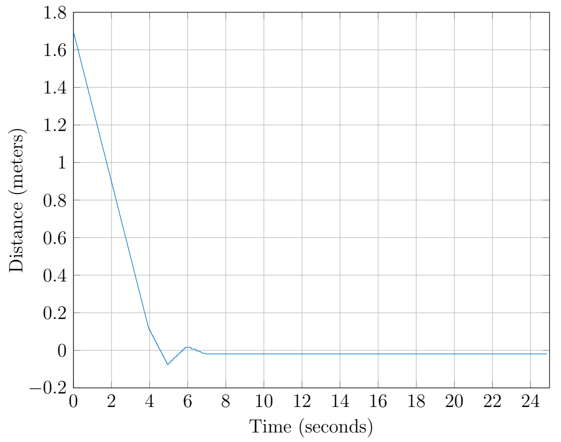


Figure 52: The error in displacement of the robot over time for $(K^R_\Psi, K^T_\omega) \equiv (0.1K^R_{\Psi,max}, 0.75K^T_{\omega,max})$

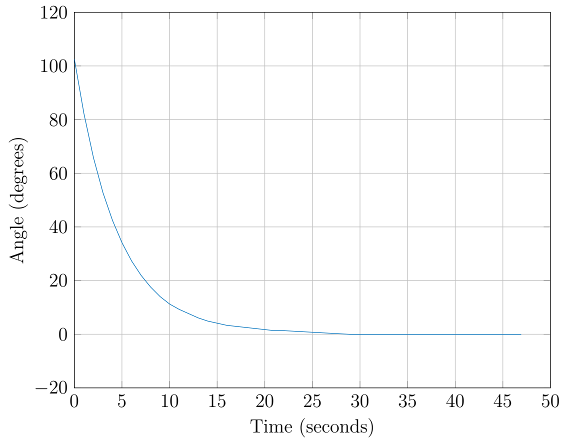


Figure 53: The error in bearing of the robot over time for $(K^R_\Psi, K^T_\omega) \equiv (0.1K^R_{\Psi,max}, 0.75K^T_{\omega,max})$

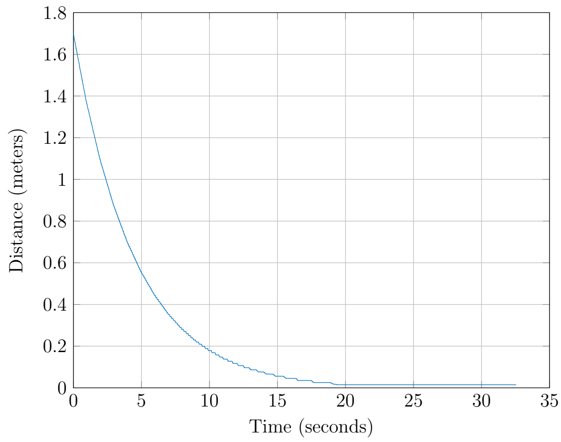


Figure 54: The error in displacement of the robot over time for $(K^R_\Psi, K^T_\omega) \equiv (0.2K^R_{\Psi,max}, 0.1K^T_{\omega,max})$

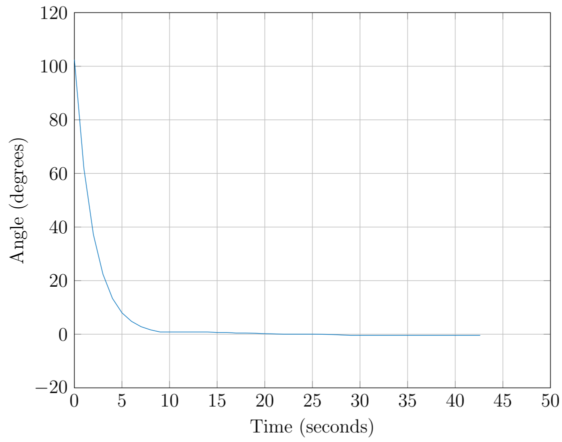


Figure 55: The error in bearing of the robot over time for $(K^R_\Psi, K^T_\omega) \equiv (0.2K^R_{\Psi,max}, 0.1K^T_{\omega,max})$

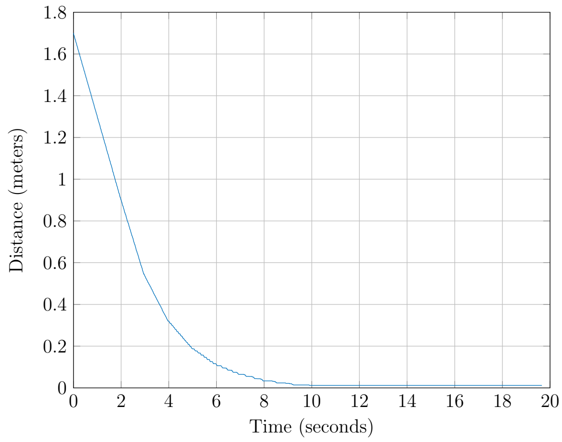


Figure 56: The error in displacement of the robot over time for $(K^R_\Psi, K^T_\omega) \equiv (0.2K^R_{\Psi,max}, 0.2K^T_{\omega,max})$

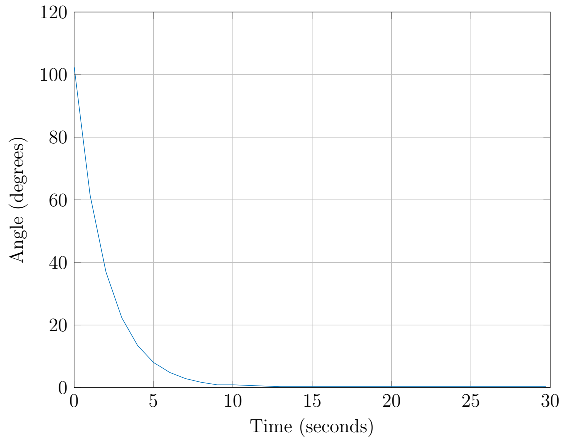


Figure 57: The error in bearing of the robot over time for $(K^R_\Psi, K^T_\omega) \equiv (0.2K^R_{\Psi,max}, 0.2K^T_{\omega,max})$

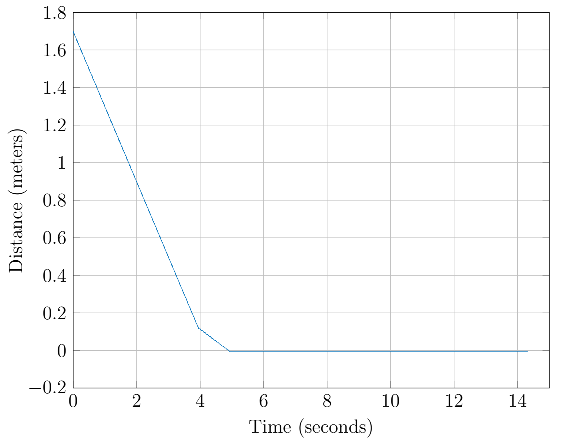


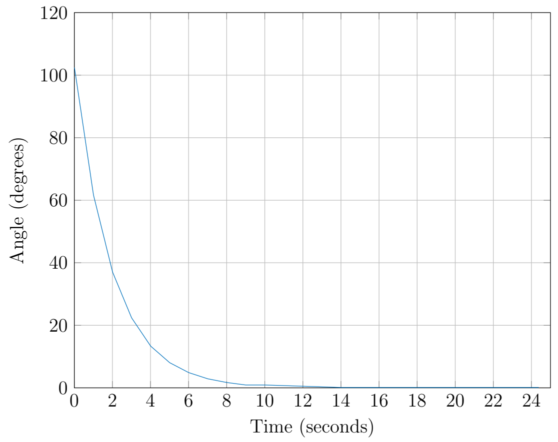


Figure 58: The error in displacement of the robot over time for $(K^R_\Psi, K^T_\omega) \equiv (0.2K^R_{\Psi,max}, 0.5K^T_{\omega,max})$

Figure 59: The error in bearing of the robot over time for $(K^R_\Psi, K^T_\omega) \equiv (0.2K^R_{\Psi,max}, 0.5K^T_{\omega,max})$

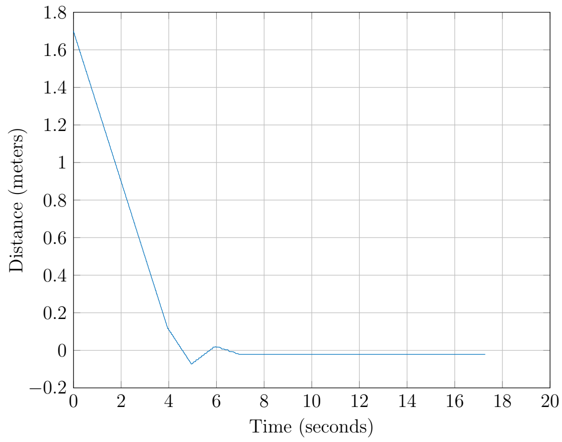


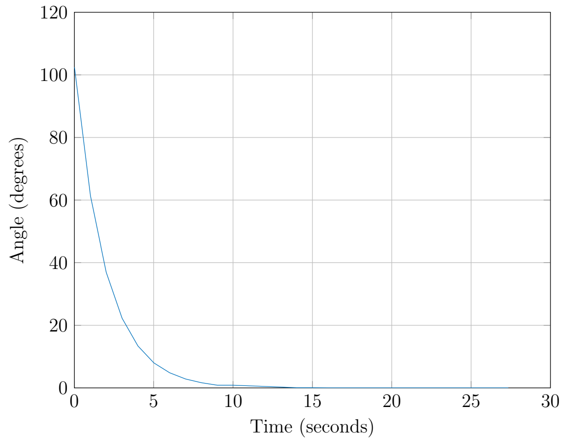


Figure 60: The error in displacement of the robot over time for $(K^R_\Psi, K^T_\omega) \equiv (0.2K^R_{\Psi,max}, 0.75K^T_{\omega,max})$

Figure 61: The error in bearing of the robot over time for $(K^R_\Psi, K^T_\omega) \equiv (0.2K^R_{\Psi,max}, 0.75K^T_{\omega,max})$

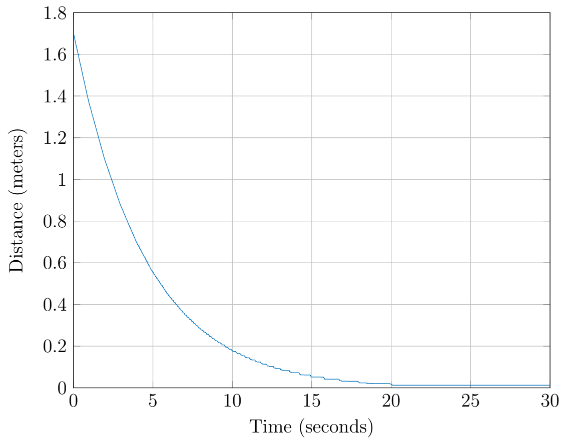


Figure 62: The error in displacement of the robot over time for $(K^R_\Psi, K^T_\omega) \equiv (0.5K^R_{\Psi,max}, 0.1K^T_{\omega,max})$

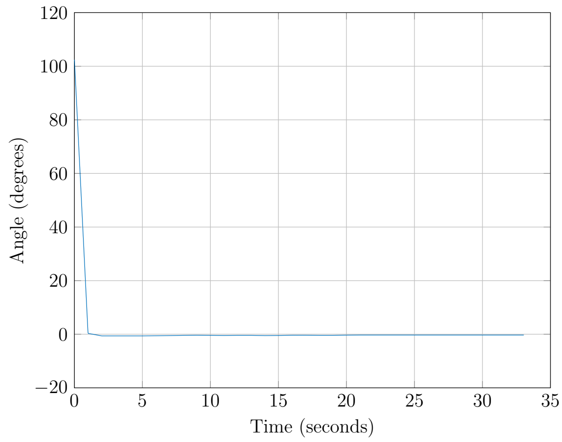


Figure 63: The error in bearing of the robot over time for $(K^R_\Psi, K^T_\omega) \equiv (0.5K^R_{\Psi,max}, 0.1K^T_{\omega,max})$

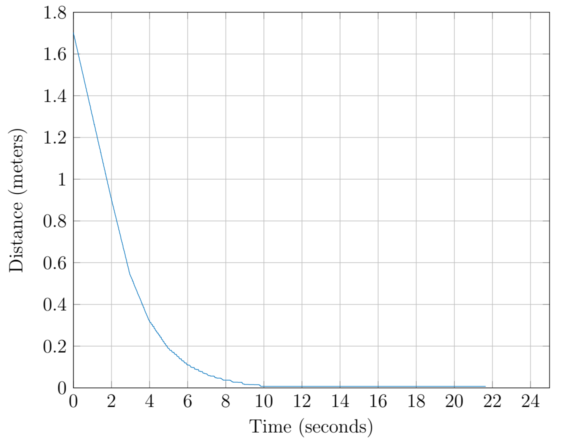


Figure 64: The error in displacement of the robot over time for $(K^R_\Psi, K^T_\omega) \equiv (0.5K^R_{\Psi,max}, 0.2K^T_{\omega,max})$

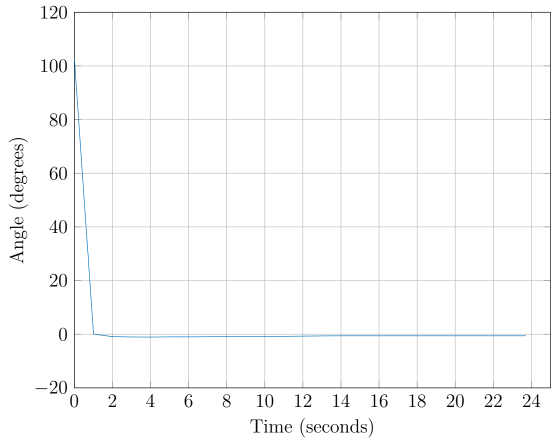


Figure 65: The error in bearing of the robot over time for $(K^R_\Psi, K^T_\omega) \equiv (0.5K^R_{\Psi,max}, 0.2K^T_{\omega,max})$

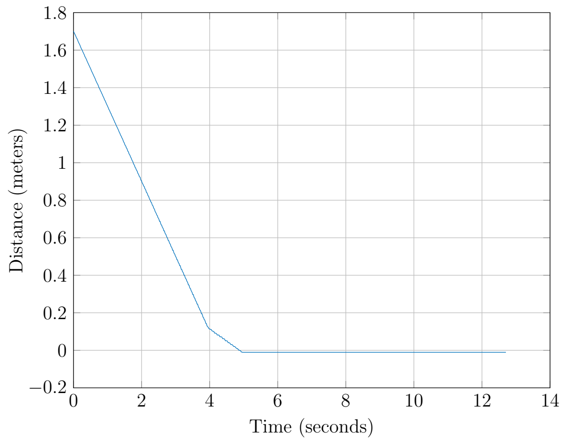


Figure 66: The error in displacement of the robot over time for $(K^R_\Psi, K^T_\omega) \equiv (0.5K^R_{\Psi,max}, 0.5K^T_{\omega,max})$

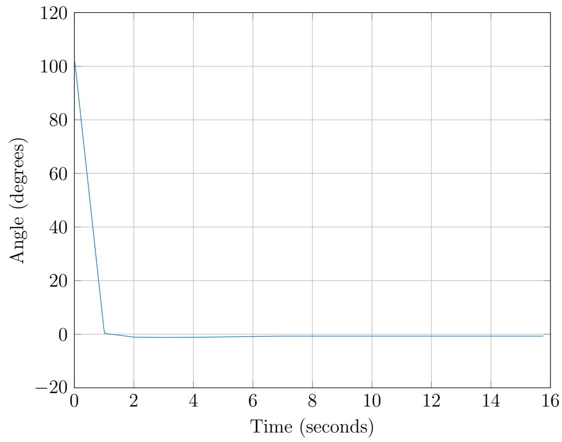


Figure 67: The error in bearing of the robot over time for $(K^R_\Psi, K^T_\omega) \equiv (0.5K^R_{\Psi,max}, 0.5K^T_{\omega,max})$

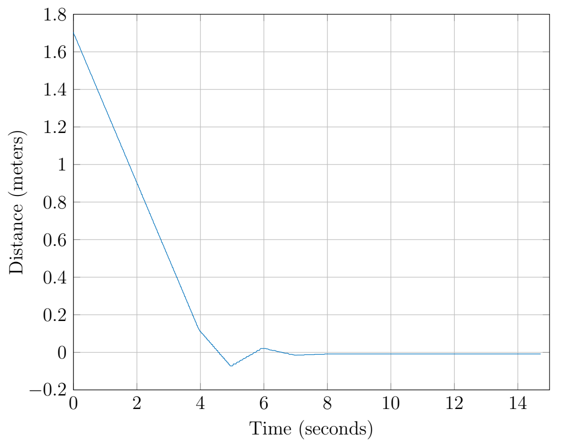


Figure 68: The error in displacement of the robot over time for $(K^R_\Psi, K^T_\omega) \equiv (0.5K^R_{\Psi,max}, 0.75K^T_{\omega,max})$

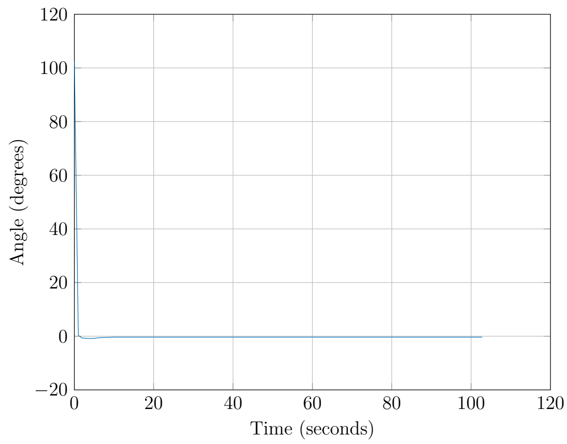


Figure 69: The error in bearing of the robot over time for $(K^R_\Psi, K^T_\omega) \equiv (0.5K^R_{\Psi,max}, 0.75K^T_{\omega,max})$

# Task 20

# Task 21

# Task 22

# References

[] Hassan K Khalil. *Nonlinear systems.* Prentice Hall, Upper Saddle river, 3. edition, 2002. ISBN 0-13-067389-7.

[] Tobias Oetiker, Hubert Partl, Irene Hyna, and Elisabeth Schlegl. *The Not So Short*

| $K^R_\Psi/K^R_{\Psi,max}$ | $K^T_\omega/K^T_{\omega,max}$ | $e_d(cm)$ | $e_\theta$(deg) |
|---|---|---|---|
| 0.1 | 0.1 | 1.73 | -0.329 |
| 0.1 | 0.2 | 0.60 | 0.144 |
| 0.1 | 0.5 | -0.90 | 0.330 |
| 0.1 | 0.75 | -1.9 | -0.054 |
| 0.2 | 0.1 | 1.47 | -0.419 |
| 0.2 | 0.2 | 1.21 | 0.308 |
| 0.2 | 0.5 | -0.67 | 0.116 |
| 0.2 | 0.75 | -2.12 | 0.026 |
| 0.5 | 0.1 | 1.26 | -0.303 |
| 0.5 | 0.2 | 0.75 | -0.585 |
| 0.5 | 0.5 | -1.05 | -0.695 |
| 0.5 | 0.75 | -0.86 | -0.347 |

Table 1:

*Introduction to LaTeX 2ε*. Oetiker, OETIKER+PARTNER AG, Aarweg 15, 4600 Olten, Switzerland, 2008. http://www.ctan.org/info/lshort/.

[] Shankar Sastry. *Nonlinear systems: analysis, stability, and control*, volume 10. Springer, New York, N.Y., 1999. ISBN 0-387-98513-1.